The Effects of Primary Blast Shock Waves on Skeletal Muscle



Robert Michal Taylor Staruch
Magdalen College
University of Oxford

Appendices

Chapter 1 Appendix Material

Appendix Contents

List of Figures

Appendix Figure 1.7: Pressure vs Time profiles of different shock waves sources.
Appendix Figure 2.1: Quality assessment of Porcine and Rabbit Bulk Sequencing data.
Appendix Figure 4.1: Design phases of printed post model
Appendix Figure 4.2: Heatmap of housekeeping genes
Appendix Figure 4.3: Bulk RNA sequence at 4 hours.
Appendix Figure 4.4: Bulk RNA sequence at 7 Days.
Appendix Figure 4.5: Molecular Output of Gene Set Enrichment Analysis (GSEA)
Appendix Figure 4.6: Cellular Output of Gene Set Enrichment Analysis (GSEA)
Appendix Figure 4.7: Top 50 Significant genes in Cluster groups 1 & 2 in the Treatment group.
Appendix Figure 4.8: Top 50 Significant genes in Cluster groups 1 & 2 in the Control group.
Appendix Figure 4.9: Gene Set Enrichment analysis data of Control and Treatment LRT gene data.

Appendix Table 1.1.: A Review of methods and results from in vivo models of blast
Appendix Table 1.2: Ex Vivo Models for Blast
Appendix Table 2.1: Nanodrop & Bioanalyzer data for a snapshot of in Vivo samples.
Appendix Table 2.2: Rabbit alignment
Appendix Table 2.3: Porcine alignment
Appendix Table 2.4: Tables outlining the sample ID's and their assigned groups in Porcine model.
Appendix Table 2.5: Tables outlining the sample ID's and their assigned groups in Rabbit model.
Appendix Table 4.1: Table outline design requirements
Appendix Table 4.2: Outline types of models used to investigate blast.

Github Repository:

R Markdowns can be found here: https://github.com/robstaruchox/Thesis

1

Appendix Figure 1.1: Pressure time profies of experimental platforms used to replicate primary blast.

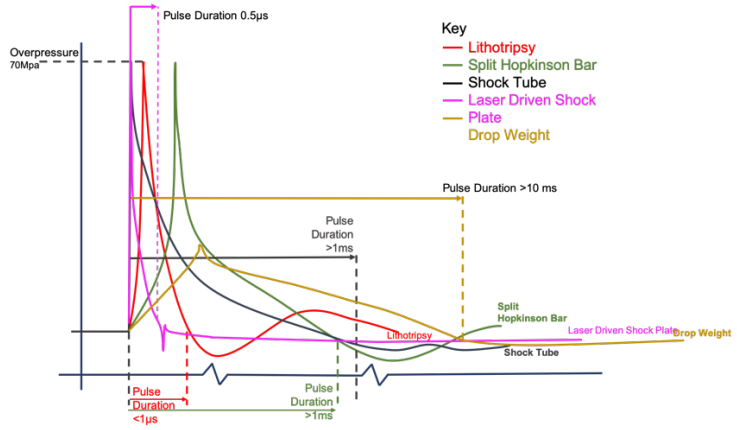

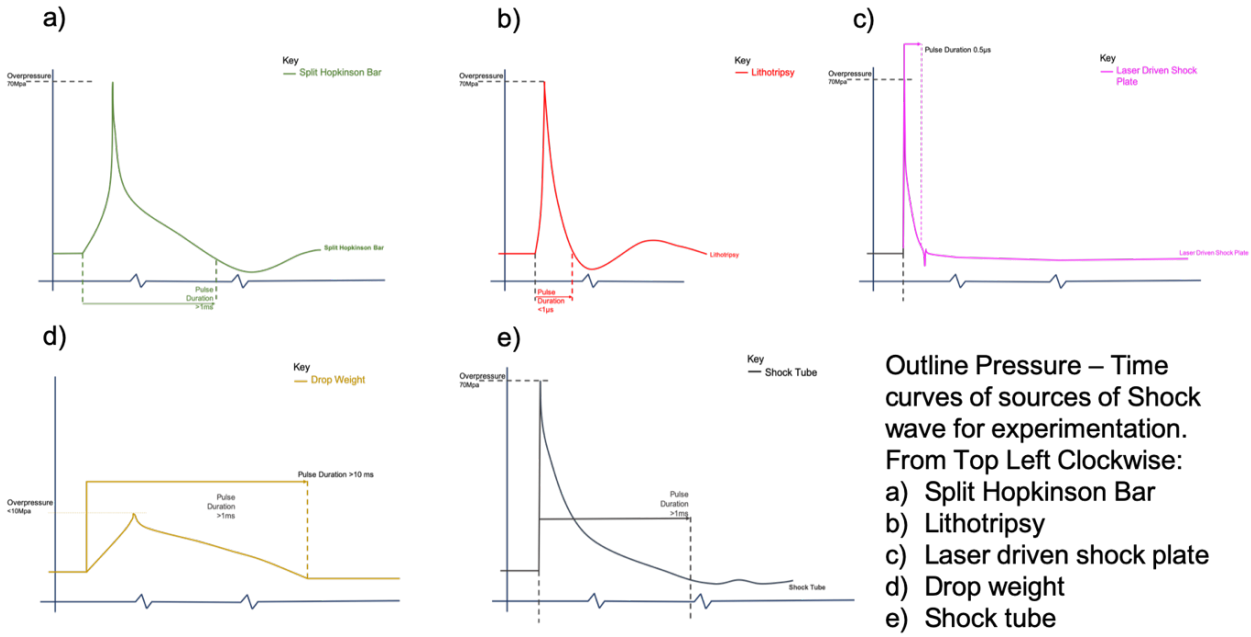

Outline Pressure – Time curves of sources of Shock wave for experimentation. From Top Left Clockwise:

a) Split Hopkinson Bar
b) Lithotripsy
c) Laser driven shock plate
d) Drop weight
e) Shock tube

Year	**Author**	**Animal**	**Source**	**Set Up**	**Outcomes**
2016	Eftaxiopoulou et al(*64*)	Rat	Compressed air driven shock tube	Anaesthetized Sprague dawley rats, Collections of blood, plasma for NK cells, Neutrophils, Monocytes and T cells. Elisa for Cytokine analysis. Liver, Lung and quadriceps samples for histology – H&E.	Focused delivery of air blast shock waves causes changes in circulating inflammatory cells and cytokines. Changes are most notably dependent on the duration of the wave. No histological damage in muscle, lung, liver.
2015	Spear et al(*65*)	Rabbit	Compressed air driven air storage cylinder with solenoid valve.	Circulating endothelial cells, plasma and excision of gastrocnemius for RT-qPCR for TNF-alpha, e-selecting, interleukin-6, thrombomodulin, hypoxia inducible factor-1, peroxisome proliferator-activated receptor-γ 1- α (PGC-1α), VEGF, platelet derived growth factor, vascular cell adhesion molecule, ET-1, erythropoietin. Histology of gastrocnemius for hemorrhage, inflammatory cell infiltration and edema and muscle fiber bundle necrosis.	Blast injury has demonstrated an ability to activate the endothelium and result in damage to surrounding tissue, such as edema and inflammatory cell infiltrate.
2013	Skotak et al(*47*)	Rat	Helium driven shock tube	Three sets of experiments. Cadaveric rats used to assess pressure on the surface of the nose, in the lungs and in the brain. The second study assessed rats immediately after injury for gross lung pathology and histology. The third study assessed physiological vital signs, heart rate, blood oxygen saturation and perfusion index for 2x30 minute periods.	Mortality rates in rats are correlated to ICP amplitude and frequency, indicating the specific response of the skull to blast loading is affecting outcome.
2012	Shridharani et al(*48*)	Pig and Ferret	Gas driven shock tube	Pigs skulls were exposed to explosively generated waveforms representative of small, medium and large IEDs. Post blast, pigs were monitored for 5 hours. Unresolved post blast apnea was treated with ventilation. Full necroptosis of organ systems and brain histopathology was performed. Blast overpressure waveforms were scaled to induce brain hemorrhage and pulmonary contusions in ferrets.	Despite overpressure and duration conditions corresponding to a scaled 50% risk of severe bleeding and apnea, no brain bleeding was found under macroscopic inspection. There was a significant pressure decrease across the skull.
2012	Wang et al(*66*)	Mice	Compressed air driven shock tube	Mice exposed to sham control and three different blast overpressures (BOP). BOP groups included a single BOP and a repeated BOPs after a 1-minute interval. In one group a third BOP was exposed after a 30-minute interval. Mice were euthanized at 4, 24, 48hrs and assessed for brain edema, total ROS in the cortex.	Repeated blast overpressure exposure increased mortality from 2 to 20%. Repeated blast exposure increased body weight loss, the duration of righting reflex time and brain edema and reactive oxygen species.
2011	Cernak et al(*67*)	Mice	Helium driven shock tube	Mice were exposed to blast of mild moderate and severe lethality. There were nine experimental groups. These measured mortality rates, injury severity categories, vital function and functional – motor cognitive and behavior outcome measurements. Inflammatory gene response at 1,3,7,14, and 30 days after exposure – looking at glial fibrillary acidic protein (GFAP), ED1, myeloid related protein 8 (MRP8), Osteopontin (OPN), Chemokine CC Ligand-2.	Model of blast brain injury capable of delivering functional and physiological injury in vivo. Significant upregulation of all tested genes in injury severity dependent manner. Results showed a potential causal relationship between inflammation and long term functional neurological deficit.
2011	Kirkman et al(*60*)	Porcine	Open Air Blast	Induction of controlled hemorrhage after blast with 5 minutes of shock phase followed by resuscitation protocol.	Hypertonic saline dextran inferior to normal saline after combined blast and hemorrhage.
2011	Tannous et al(*68*)	Rats	Water Based Pentaerythritol tetranitrate explosion	Sprague dawley rats underwent forelimb or hindlimb amputation from exposure to blast and wounds were washed and closed. Primary outcome measure was radiographic presence of heterotopic ossification (HO).	All four surviving animals exhibited Type A bone growth, ¾ exhibited non-contiguous islands of heterotopic bone. One exhibited ectopic bone HO types ‘A’ & ‘B’ within soft tissue injury.
2010	Cheng et al(*69*)	Rat	Piezoelectric Detonation Chamber	Rats sealed in aluminum casing with head exposed through opening to electronic detonation. Physiological and neurobehavioral indices were recorded. Histopathologic changes, neuron specific enolase expression changes and tissue water content was examined.	Changes of brain tissue water content, 87% of rats developed apnea, limb seizure, poor appetite, limpness. Diffuse subarachnoid hemorrhage and edema in brain parenchyma.
2010	Satoh et al(*70*)	Mice	Laser Induced Stress Waves	neodymium-doped yttrium aluminum garnet (Nd: YAG) laser induced stress waves were coupled to rubber on mice chest walls, with four low intensity shock waves to cover the area of the lungs. Physiological outcomes	Non-lethal doses of laser shock waves caused pulmonary contusions with hemorrhages depending on peak pressure. Model suitable for studies of blast lung contusion.

				including peripheral oxyhemoglobin, heart rate and mean arterial pressure for 60 minutes post injury.	
2008	Saljo et al(*71*)	Porcine	Air driven shock tube & underwater apparatus. Live munitions used to generate overpressure effects.	Pigs were exposed to either air blast, underwater blast or localized blast. Histological assessment of porcine brains after exposure.	Significant small hemorrhages in the posterior parts of the brains. As expected attenuation was stronger in water. Little evidence from data to show that there is significant spread of pressure within the body.
2006	Chavko et al(*72*)	Rats	Compressed air driven Shock Tube	Blast injury severity measured using the pathology scoring system for blast injuries. (*73*) Rats were then assessed for histopathological changes with H&E. Lung tissue was assessed for neutrophil activity, oxidative stress and protein oxidation and protein nitration.	Blast overpressure showed the role of adaptive anti-oxidant and anti-inflammatory mechanisms in lung recovery.
1954	Clemedson et al(*74*)	Rabbit	Detonation Chamber	Lung Injury – particularly the phase of the respiration and the degree of lung injury.	Correlation between respiratory phase and lung damage in blast injury and the mechanics of breathing during detonation.

Appendix *Table 1.1.:* *A Review of methods and results from in vivo models of blast*

Model Type	Advantages of Model	Disadvantages of Model	Examples
Tissue Slice	*Cells remain in their native architecture & orientation.* *Advantageous for understanding the effects of loading on bulk tissue properties.* ***Well-established protocols exist for certain tissue types (e.g. brain).***	*Tissue has to undergo surgical trauma to remove it from native environment.* **tissue slice utilizes are de vascularized, making deductions about role of vasculature or diffusion of nutrients into environment more difficult.** *Although cell-cell/cell-ECM spatial relationships are maintained, such systems (particularly brain) lose their functional output after slicing.* **Limited extended culture time (3-7 days)**	Hippocampal slice,(*30, 31*) Ex Vivo rat spinal cord. (*23*) Lung & Liver (*75-79*)
Perfused tissue/ organ models	*Allows investigation of whole tissue function whilst perfused.* **Enables real time monitoring of physiological endpoints/ markers of injury at tissue level.** *Allows characterization of tissue homeostasis as a hierarchical structure.* **Valuable for evaluating the role vasculature/ microvasculature has in organ/cell function.**	More challenging to undertake in depth cellular characterization from whole tissue – requires biopsy then culture. Expensive systems to run – requiring blood/ perfusion fluid and monitoring/human + machine Limited tissue viability time (in a true physiological state) – c. 24 hr.	Ex Vivo Hindlimb. (*80-82*) (For CTA). (*83*)
	Experimental outputs similar to in vivo models for experimental/pre-clinical value. **Reduced cost compared to in vivo work.** *Allows evaluation of whole organ/ extremity response to trauma.*		

Appendix Table 1.2: Ex Vivo Models for Blast

2

Chapter 2 Appendix

Table 2.1: Nanodrop & Bioanalyzer data for a snapshot of in Vivo samples.

	Nanodrop			**Bioanalyzer**
Sample	ng/ul	260/280	260/230	RIN
2-A4	75.7	2.05	1.59	10
2-D4	48.6	2.04	1.36	9.2
2-E4	70.8	2.04	1.5	10
2-A5	85.95	2.06	0.58	9.6
2-B5	37	2.11	0.42	9.8
2-C5	97	2.05	0.5	9.8
3-B7	27.7	2	0.68	9
1-D7	24.1	2.12	0.45	9.4

Table 2.2 Rabbit Alignment

Sample ID	Raw Reads (Paired)	Alignment
RPFN1 _Run1	38,823,461	82.85
RPFN1 _Run2	19,597,459	82.43
RPFN2 _Run1	39,448,385	83.91
RPFN2 _Run2	20,963,748	83.46
RPFN3 _Run1	43,222,947	83.73
RPFN3 _Run2	22,788,697	83.27
RPFN4 _Run1	38,963,424	81.36
RPFN4 _Run2	19,592,250	80.95
RPFN5 _Run1	43,109,557	82.40
RPFN5 _Run2	22,507,522	81.94
RPFN7 _Run1	43,173,782	79.79
RPFN7 _Run2	22,481,739	79.37
RPFN8 _Run1	37,610,231	84.09
RPFN8 _Run2	19,527,163	83.65
RPFN9 _Run1	47,575,654	83.45
RPFN9 _Run2	25,096,693	82.95
RPFN11 _Run1	40,654,959	83.01
RPFN11 _Run2	21,079,980	82.55
RPFN12 _Run1	52,244,999	85.39
RPFN12 _Run2	27,704,570	84.72
RPFN17 _Run1	44,036,826	85.32
RPFN17 _Run2	21,863,766	84.88
RPFN20 _Run1	43,210,495	81.26

RPFN20 _Run2	22,692,603	80.82
RPFN23 _Run1	35,872,864	80.45
RPFN23 _Run2	18,501,331	80.01
RPFN24 _Run1	39,162,088	83.97
RPFN24 _Run2	19,434,457	83.60
RPFN25 _Run1	40,574,404	79.81
RPFN25 _Run2	21,389,817	79.10
RPFN28 _Run1	39,547,186	83.53
RPFN28 _Run2	20,596,720	83.14
RPFN29 _Run1	37,755,648	82.73
RPFN29 _Run2	19,152,425	82.28
RPFN33 _Run1	37,721,661	83.14
RPFN33 _Run2	19,709,347	82.70
RPFN35 _Run1	37,542,138	85.15
RPFN35 _Run2	19,320,368	84.72
RPFN36 _Run1	41,735,305	83.89
RPFN36 _Run2	21,636,311	83.43
RPFN37 _Run1	40,012,704	85.07
RPFN37 _Run2	21,067,782	84.66
RPFN38 _Run1	39,210,226	84.10
RPFN38 _Run2	20,533,202	83.68

Table 2.3 Porcine Alignment

Sample ID	**Raw reads (paired)**	**Alignment (%)**
HR61_Run1	37,589,199	83.90
HR61_Run2	42,789,813	86.32
HR62_Run1	46,880,340	90.41
HR62_Run2	51,551,475	87.10
HR66_Run1	35,011,612	77.05
HR66_Run2	41,228,675	87.76
HR70_Run1	54,442,497	89.86
HR70_Run2	55,699,343	90.45
HR71_Run1	41,937,779	87.76
HR71_Run2	50,257,363	90.35
HR74_Run1	53,331,480	90.08
HR74_Run2	62,961,166	92.93
HR78_Run1	34,462,526	79.22
HR78_Run2	46,297,720	93.77
HR80_Run1	46,809,094	85.93
HR80_Run2	47,960,388	86.92
HR81_Run1	21,963,894	86.02
HR81_Run2	46,025,127	86.61
HR86_Run1	46,584,909	83.42

HR86_Run2	47,904,254	88.18
HR87_Run1	18,610,335	83.44
HR87_Run2	26,047,145	89.98
HR99_Run1	26,338,690	86.46
HR99_Run2	29,754,113	89.96
HR107_Run1	18,131,585	76.84
HR107_Run2	20,941,962	87.58
HR114_Run1	21,842,299	87.36
HR114_Run2	28,038,472	89.34
HR115_Run1	24,152,306	93.68
HR115_Run2	26,632,730	89.93
HR121_Run1	28,437,729	89.61
HR121_Run2	33,289,366	92.53
HR127_Run1	17,974,276	78.86
HR127_Run2	24,442,155	85.31
HR142_Run1	25,318,559	87.64
HR142_Run2	25,821,592	86.46
HR146_Run1	22,992,472	86.35
HR146_Run2	25,155,974	83.02

Table 2.4 & 2.5: Tables outlining the sample ID's and their assigned groups.

Pig

ID	Group	Test
HR62	A	Control
HR70	A	Control
HR78	A	Control
HR81	A	Control
HR87	A	Control
HR99	A	Control
HR107	A	Control
HR114	A	Control
HR61	B	Blast
HR66	B	Blast
HR71	B	Blast
HR74	B	Blast
HR80	B	Blast
HR86	B	Blast
HR115	B	Blast
HR121	B	Blast
HR127	B	Blast
HR142	B	Blast
HR146	B	Blast

Rabbit

ID	Group	Test
RPFN1	H	Blast
RPFN3	H	Blast
RPFN5	H	Blast
RPFN7	H	Blast
RPFN9	H	Blast
RPFN11	H	Blast
RPFN12	H	Blast
RPFN23	H	Blast
RPFN25	H	Blast
RPFN33	H	Blast
RPFN36	H	Blast
RPFN38	H	Blast
RPFN2	S	Control
RPFN4	S	Control
RPFN8	S	Control
RPFN17	S	Control
RPFN20	S	Control
RPFN24	S	Control
RPFN28	S	Control
RPFN29	S	Control
RPFN35	S	Control
RPFN37	S	Control

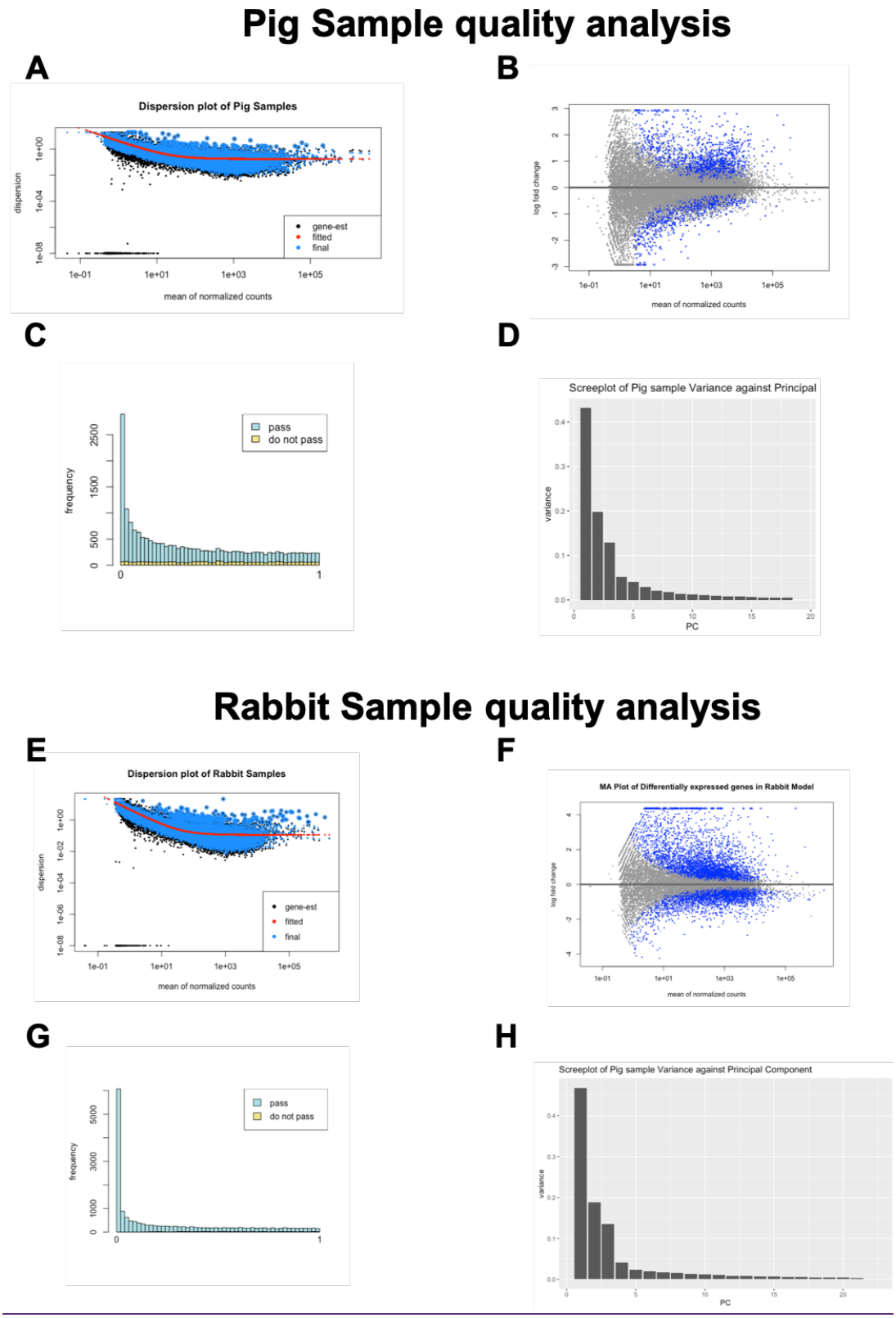

Figure 2.1: Quality assessment of Porcine and Rabbit Bulk Sequencing data.

3

Chapter 3 Appendix

Ovid Medline search strategy

Database: Medline (Ovid MEDLINE® Epub Ahead of Print, In-Process & Other Non-Indexed Citations, Ovid MEDLINE® Daily and Ovid MEDLINE®) 1946 to present

Search Strategy: (03/12/2021)

---

1 exp Myoblasts, Skeletal/ (3767)

2 (skeletal adj2 myoblast*).tw. (1665)

3 (cell* adj2 (stem or primary or satellite)).tw. (354740)

4 (myogenic or skeletal muscle).tw. (124132)

5 3 and 4 (6997)

6 Muscle, Skeletal/ (152759)

7 Muscle Fibers, Skeletal/ (16240)

8 Muscle Fibers, Slow-Twitch/ (2423)

9 Muscle Fibers, Fast-Twitch/ (3070)

10 skeletal.tw. (211337)

11 (muscle* adj2 fiber*).tw. (27457)

12 10 and 11 (10275)

13 (fast-twitch or intermediate or white or type II).tw. (737952)

14 (red or slow-twitch or type I).tw. (435930)

15 13 or 14 (1110199)

16 11 and 15 (5086)

17 myotube*.tw. (11260)

18 (skeletal adj2 myocyte*).tw. (546)

19 (myogenic or skeletal muscle).tw. (124132)

20 (cell* adj2 c2c12).tw. (3969)

21 19 and 20 (2116)

22 1 or 2 or 5 or 6 or 7 or 8 or 9 or 12 or 16 or 17 or 18 or 21 (178008)

23 3d.tw. (186689)

24 three d.tw. (432)

25 3 dimension*.tw. (25671)

26 Organoids/ (11114)

27 organoid*.tw. (8229)

28 Lab-On-A-Chip Devices/ (6197)

29 "lab on a chip".tw. (2763)

30 "organ on a chip".tw. (555)

31 exp Bioengineering/ (53782)

32 bioengineer*.tw. (8670)

33 biological engineer*.tw. (349)

34 Tissue Engineering/ (39754)

35 tissue engineer*.tw. (48806)

36 23 or 24 or 25 or 26 or 27 or 28 or 29 or 30 or 31 or 32 or 33 or 34 or 35 (300040)

37 22 and 36 (2817)

Ovid Embase:

Database: Embase 1974 to present

Search Strategy: (03/12/2021)

---

1 *skeletal myoblast/ (108)

2 skeletal myoblast/ (430)

3 (skeletal adj2 myoblast*).tw. (1966)

4 *skeletal muscle cell line/ (10)

5 skeletal muscle cell line/ (40)

6 (cell* adj2 (stem or primary or satellite)).tw. (519094)

7 (myogenic or skeletal muscle).tw. (148935)

8 6 and 7 (8960)

9 *skeletal muscle/ (44929)

10 skeletal muscle/ (126452)

11 *slow muscle fiber/ (565)

12 slow muscle fiber/ (1991)

13 *fast muscle fiber/ (634)

14 fast muscle fiber/ (2075)

15 skeletal.tw. (259975)

16 (muscle* adj2 fiber*).tw. (31705)

17 15 and 16 (11987)

18 (fast-twitch or intermediate or white or type II).tw. (956554)

19 (red or slow-twitch or type I).tw. (549569)

20 18 or 19 (1426310)

21 16 and 20 (5933)

22 myotube*.tw. (13588)

23 (skeletal adj2 myocyte*).tw. (667)

24 (myogenic or skeletal muscle).tw. (148935)

25 (cell* adj2 c2c12).tw. (5228)

26 24 and 25 (2803)

27 1 or 3 or 4 or 8 or 9 or 11 or 13 or 17 or 21 or 22 or 23 or 26 (75846)

28 2 or 3 or 5 or 8 or 10 or 12 or 14 or 17 or 21 or 22 or 23 or 26 (150065)

29 3d.tw. (247214)

30 three d.tw. (560)

31 3 dimension*.tw. (33087)

32 exp *organoid/ (3685)

33 exp organoid/ (8171)

34 organoid*.tw. (12174)

35 exp *lab on a chip/ (3548)

36 exp lab on a chip/ (7050)

37 "lab on a chip".tw. (2669)

38 "organ on a chip".tw. (556)

39 exp *bioengineering/ (86464)

40 exp bioengineering/ (194214)

41 bioengineer*.tw. (11557)

42 biological engineer*.tw. (1295)

43 *tissue engineering/ (26420)

44 tissue engineering/ (57216)

45 tissue engineer*.tw. (58365)

46 29 or 30 or 31 or 32 or 34 or 35 or 37 or 38 or 39 or 41 or 42 or 43 or 45 (405361)

47 29 or 30 or 31 or 33 or 34 or 36 or 37 or 38 or 40 or 41 or 42 or 44 or 45 (490459)

48 27 and 46 (1745)

49 28 and 47 (3030)

50 exp *injury/ (1098483)

51 exp injury/ (2357627)

52 (injur* or wound*).tw. (1364233)

53 50 or 52 (1940999)

54 51 or 52 (2824059)

55 48 and 53 (324)

56 49 and 54 (646)

Web of Science search terms:

(((ALL=("Myotube" OR "Myoblast" OR "Skeletal Muscle " OR "Skeletal muscle myotube " OR "Fast twitch muscle fiber " OR "Slow twitch muscle fiber")) AND ALL=("In vitro ")) AND ALL=("tissue engineer*" OR "bioengeer*" OR "Organ on a chip" OR "Lab on a chip " OR "Organoid" OR "Three dimension* " OR "3d")) AND ALL=("injury")

4

Chapter 4 Appendix

Model optimisation

The detailed design requirements and considerations that influenced the methodology for generating the skeletal muscle hydrogel are outlined in the appendices (Table 4.2). Figure 4.1 shows images correlating with the models described in Appendix Table 4.1. As outlined in the introduction, the initial experimental strategy was to use the split hopkinson bar system to explore the effects of strain rate on cellular signalling using the model.

In optimising the model for use on the shock tubes, a higher throughput approach was required. Again, a 3D printed insert was investigated (4.1(d)), however this resulted in leakage of the cell-hydrogel mixture around the printed jig. This lead to sub-optimal hydrogel formation. This technique was therefore abandoned in favour of casting PDMS moulds within cell culture plates using a custom made jig (Fig 4.2(e) CAD image). In brief, liquid PDMS elastomer and curing agent were mixed and then syringed into the bottom of a well. Then the custom jig was placed in the well and cured at 80°C for 1 hour then left overnight on the bench. The next day the jig was removed, and a PDMS mould remained (Fig 4.2(f)). This was adopted for the first set of shock tube trials, and then further optimised to an entire custom silicone moulding plate. The plate was manufactured from metal moulds and food grade silicone (PLASTSIL) was used to cast the moulds. This system greatly improved the ease at which the model could be manufactured. As a reflection of this, over 500 individual hydrogels were cast for the shock tube trials using this method.

Model Description	Design requirement	Outline Method	Advantages	Disadvantages
Flexible Resin Button (A)	Hydrogel to fit within cylinder for Split Hopkinson bar apparatus. Dimensions 12.7mm x 12.7mm	Button printed with posts inside. Hydrogel cast round posts	Would allow for hydrogel to be neatly encapsulated for use in SPHB system.	Couldn't achieve cytocompatibility with flexible resin alone. Material properties may create impedance mismatch with SPHB bars
Flexible Resin mini posts (B)	Hydrogel to be cast round dog bone shaped posts to fit in SPHB	Hydrogel cast in cell culture plate.	Keeps material requirements (Fibrinogen/thrombin) low. High throughput manufacture (48/96 well plate)	Couldn't achieve cytocompatibility. Design was unstable in cell culture plate. Requires holder
3D post Jig (C)	Reduce volume of hydrogel in order to get orientation round posts	Jig holder for posts constructed to allow seeding of gel around posts in small volumes. Jig is then removed to leave hydrogel round posts	Reduces consumable requirement for hydrogel model. Creates reproducible method for manufacture	Jig needs to be wrapped in paraffin tape to stop fluid leakage, or sealed with fibrin gel prior to casting.
Biocompatible resin (D) Basket Jig	Ability to cast gels in cell culture plates that can then subsequently be removed and moved.	3D printed basket is lowered into the well with posts. Side walls are lowered onto basket base with posts to create smaller well to cast gel into.	Allows easy handling of posts and hydrogel system in wells of cell culture plate. Can be scaled depending on cell culture well size. Can be printed from biocompatible resin	Convoluted method for manufacturing hydrogel. Number of working parts reduced throughput of manufacture. Not formally tested with in vitro culture.
Biocompatible resin (E) Well insert holder	Insert to cell culture plate to hold	Jig is inserted into base of well, then posts are placed in gap to hold posts. Hydrogel casted in well around posts.	Simple adjunct to enable hydrogel casting in well. Jig can be scaled for different well sizes	Leakage of hydrogel fluid underneath the jig reduces amount of hydrogel that crosslinks around posts.
PDMS moulded plate (F)	Mould cell culture plate to ensure maximum hydrogel crosslinks around posts.	3D printed insert is placed in plate well, then PDMS silicone is poured around insert and cured at 80 degrees.	Simply method to adapt standard cell culture plates for hydrogel manufacture. PDMS can be sterilised with ethanol and PBS. PDMS is bio inert	Requires high volume of PDMS, which is expensive. Non uniform manufacture – produces imperfections which influence hydrogel production.
Silicone casted plate (G)	Custom cell culture plate with in built holder for posts is cast out of food grade silicone.	3D printed posts are placed in sterile silicone plate. Hydrogel mixture with cells is cast into well around posts. Posts and hydrogel can then be removed and placed in culture well plate.	Plate manufactured from metal moulds – ensuring repeatable and accurate manufacture. Silicone is easy to sterile with ethanol and PBS. Ensures repeatable hydrogels manufacture. Ensures fast production	Requires large volume of ethanol and PBS to sterile. Gels must be 'popped' out of well after synthesis, can result in damage to hydrogel itself.
Suspended posts (H)	Posts are suspended upside down in well to allow microscope imaging in plate and improved hydrogel remodelling.	3D printed posts on rectangle hanger are suspended over wells with cell-hydrogel mixture.	Hanging posts reduce need for jig within well to hold posts. Easy to integrate with cell culture plates. Multiple materials can be used to synthesis posts. Already available as off the shelf silicone product (ref Company).	Not optimised formally in vitro in order to validate methodology.

Appendix Table 4.1 Table outlining design requirements and decisions on model development. The table outlines the design requirement from each iteration, followed by the advantages and disadvantages of each attempt.

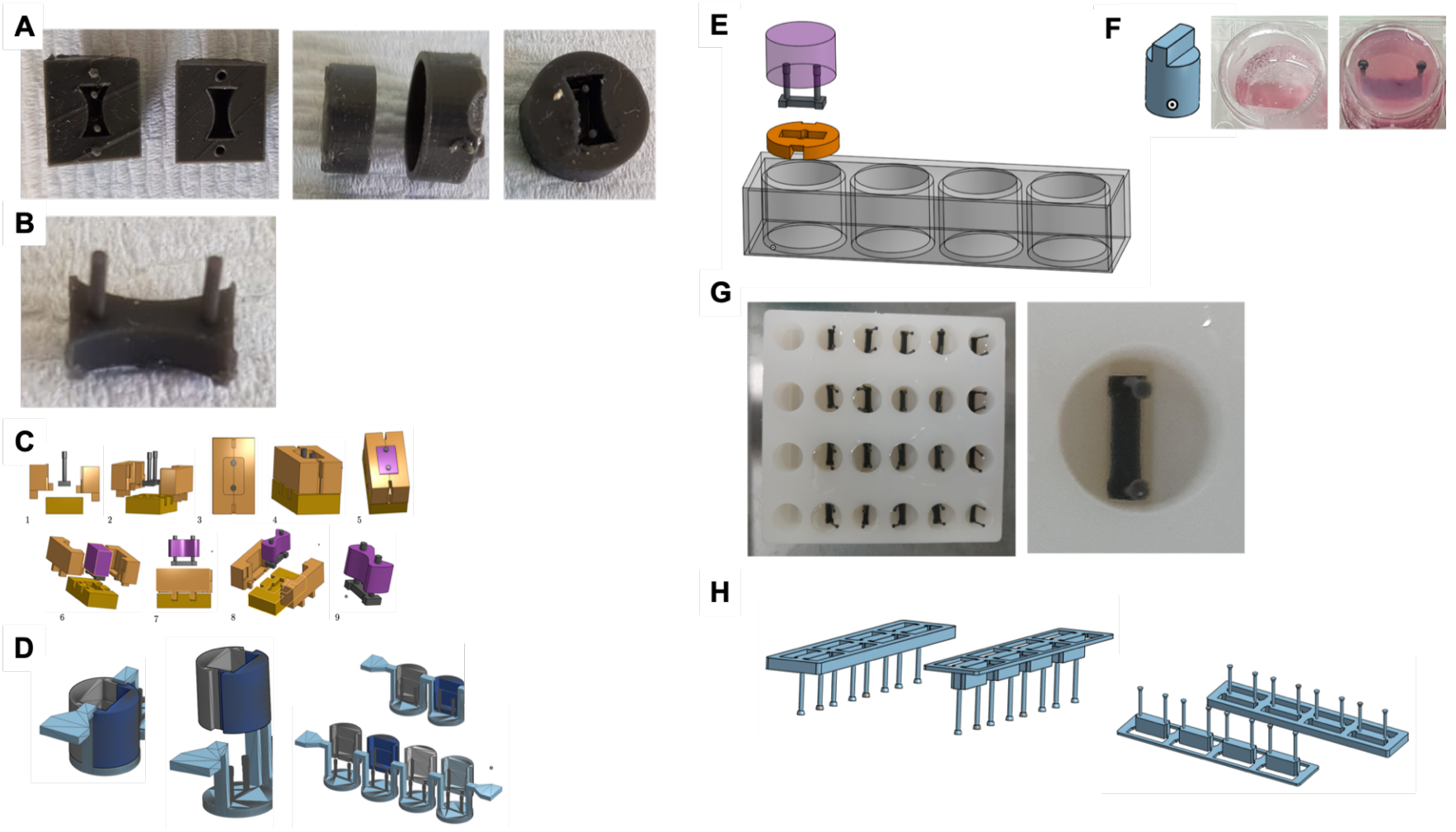

Appendix Figure 4.1: Figures A-H outlines the design phases of the printed post model.

Appendix Figure 4.1 Figure Legend: A. Shows Mark I of model designed and printed to fit in the sample gap of the Split Hopkinson bar system at the Impact Engineering Laboratories under Professor Clive Siviour, University of Oxford. **B.** Identifies Mark II of the model that created a freestanding dog bone shaped carrier to the posts and hydrogel system. Again the system is designed to fit into the Hopkinson Bar system. **C.** Demonstrates the Mark III system. This involved the creation of a casting jig to enable synthesis of the hydrogel around the printed posts. The schematic shows the process of hydrogel synthesis. **D.** Outlines the Mark IV system that employed a basket system to synthesis the hydrogel within a 12 well cell culture plate. **E.** Outlines Mark V utilised a printed implant inside the well to hold the posts for hydrogel casting. **G.** Adopting the concept in (E), a silicone system was developed with Dstl to hold and cast hydrogels in bulk. **H.** Outlines a modification of a published system to cast hydrogels using posts suspended from above.

System	Comments	Conclusion
Split Hopkinson Bar Apparatus	Unable to load whole plate of cell culture Single sample per experiment/firing Low throughput	Requires individual hydrogels that can be manipulated/utilised/tested
Drop Weight Impact Apparatus	Impact apparatus could load entire plate, but may produce inconsistent loading on individual wells (due to wave reflections).	Requirement for custom cell culture plate or individual hydrogels for experiment.
Lithotripter	Application of shock waves from lithotripter has been applied to tissue culture flasks and individual wells of cell culture plate. Altering focal zone of lithotripter enables this flexibility.	Individual hydrogel samples would allow flexibility to optimise how to use lithotripter to stimulate model – in plate, individual holder or flask.
Shock Tubes	Whole cell culture plates can be placed in an appropriately scaled shock tube. Loading therefore on whole plate, with potentially similar loading inconsistencies as with drop weight devices	Individual control of hydrogels would allow broad use for imaging, analysis and testing. Stimulating whole plate would make model higher throughput.

Appendix Table 4.2 - Outline of types of models that can be employed to investigate the mechanical effects of blast shock waves and high strain rate injury (outlined in Chapter 1) and the considerations of building a 3D model to use in these systems for experimental work.

Addendum to explain model choices in further detail

The pandemic, working restrictions and the availability of the shock tube at Dstl influenced the refocus on the experimental strategy. Appendix Table 4.2 therefore outlines the approach to designing individually manufactured hydrogels for the original experimental approach. The initial approach to hydrogel design can be seen in the first four models. The first approach was to culture the hydrogel within a button of set dimensions. The split hopkinson bar system has a predetermined sample size (12.7mm x 12.7mm cylinder). Hence the initial approach was to design an entire mould that the hydrogel could be cultured within. The limitation of this technique was the lack of biocompatibility of the flexible resin. To circumvent this, along with the impedance mismatch of the resin against metal bars, a metal sample holder was designed to hold the hydrogel system. Therefore, the next iteration need only be the development of individual skeletal muscle hydrogel systems. This is represented by Figure 4.2(D) & 4.2(D) . Figure 4.2(C) shows a combined 3D printed jig and post system. In this iteration, a set of posts was encapsulated in a jig that encased the liquid hydrogel and cell mixture round the posts until it crosslinked. Then the jig was released away from the hydrogel to leave the construct. This is outlined in Fig 4.2(C). Although this appeared a practical approach, in order to prevent leakage of the cell-hydrogel mixture from the jig, it was necessary to wrap it in parafilm or use hydrogel to pre seal the jig prior to casting. This meant that the process of casting one gel became cumbersome and low throughput. Furthermore, the system required large amounts of 3D printing resins, as well as printing time .This system, and that outlined in Fig 4.2(D) were therefore abandoned.

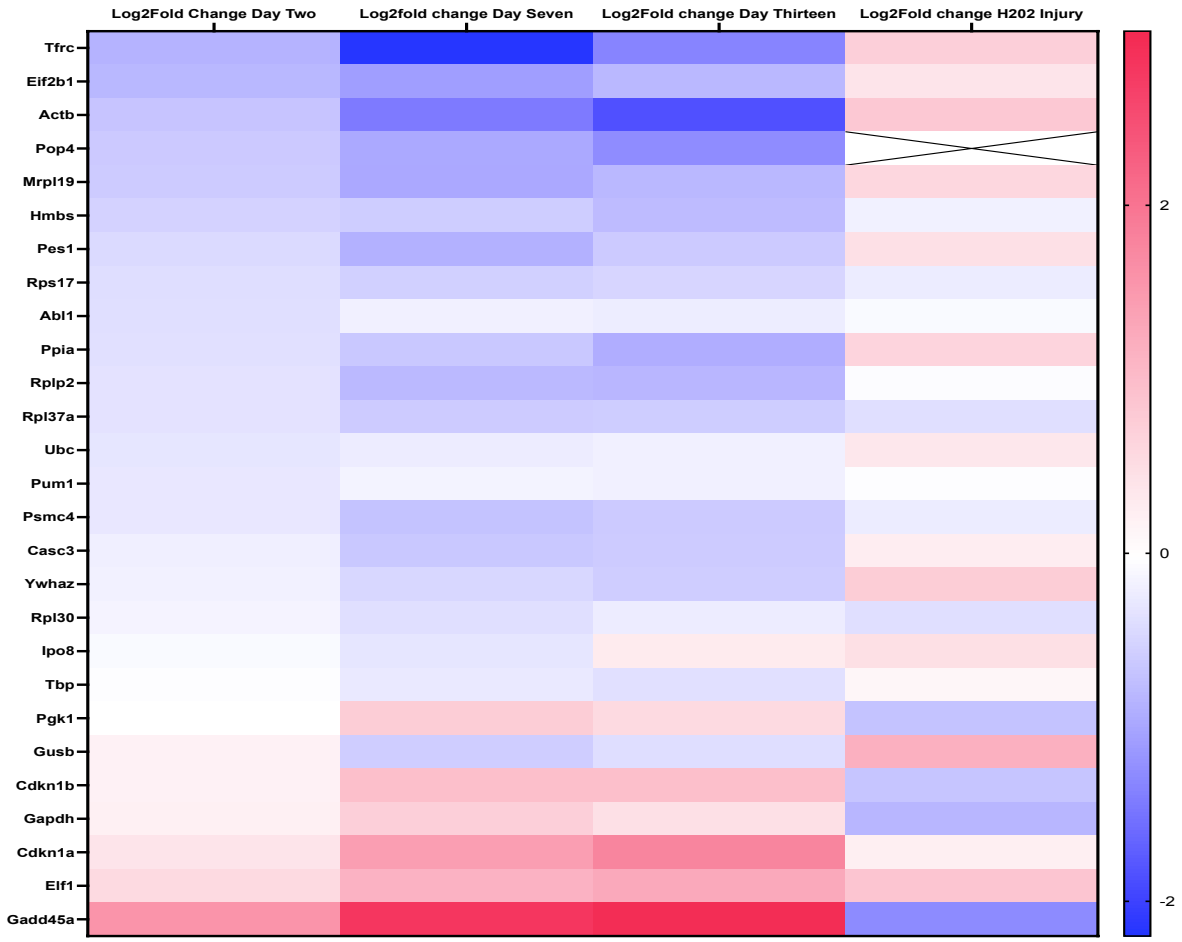

Appendix Figure 4.2 – Heatmap of housekeeping gene expression across samples. As outlined in the methods, a list of endogenous control genes for mouse experiments was adopted from a Taqman kit. The results of thee sequencing data was then probed with this gene list to identify log2fold expression and significance. None of the endogenous controls achieved significant expression across timepoints.

4 Hour Analysis - Results

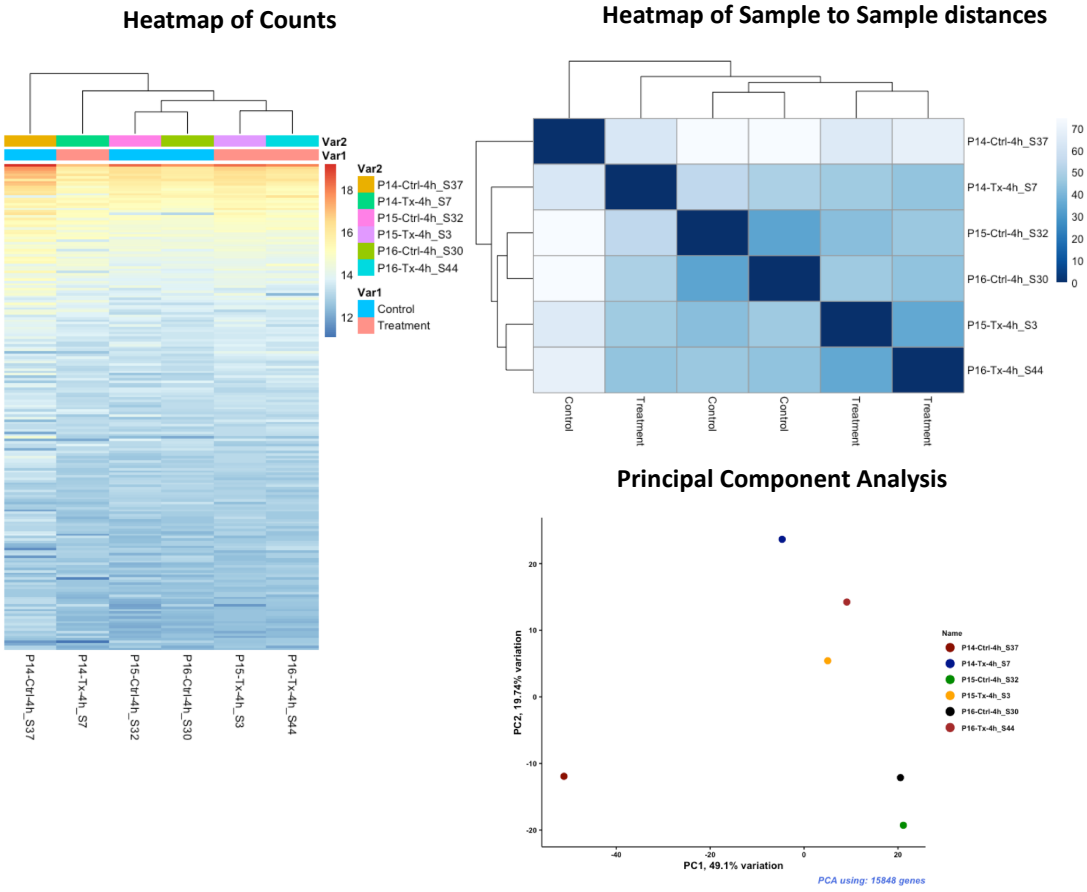

Appendix Figure 4.3 – Data from the bulk RNA sequence analysis of samples at 4 hours. The Figure presents the heatmaps of normalised counts for the top 50 genes in each sample. It presents the heatmap of sample to sample distances for treatment and control samples and annotations of cluster dendrograms between samples. Finally the principal component analysis of samples is shown. The PC1 variation is 49.1%.

Day 7 Analysis - Results

Heatmap of Counts

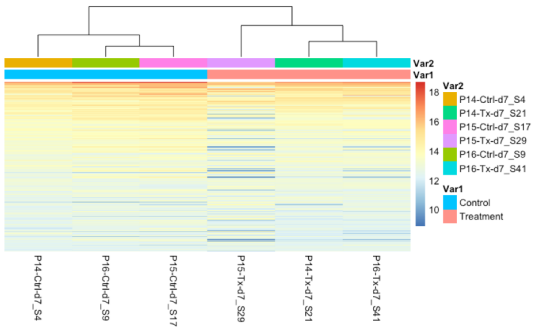

Heatmap of Sample to Sample distances

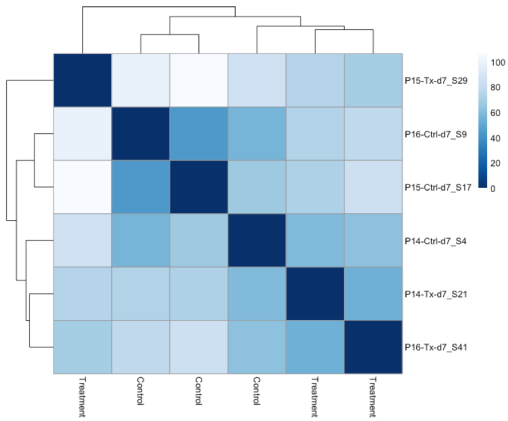

Volcano Plot of Expression at 7 Days

Principal Component Analysis

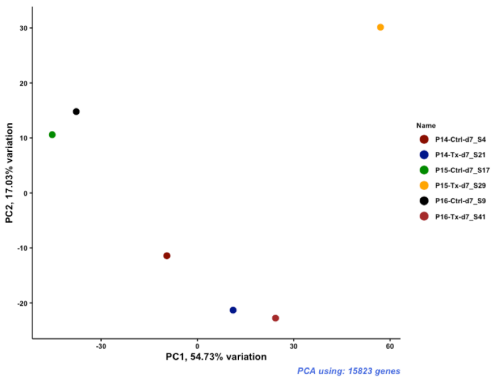

Appendix Figure 4.4 – Data from the bulk RNA sequence analysis of samples at 7 days. The Figure presents the heatmaps of normalised counts for the top 50 genes in each sample. It presents the heatmap of sample to sample distances for treatment and control samples and annotations of cluster dendrograms between samples. Finally the principal component analysis of samples is shown. The PC1 variation is 54.7%.

Molecular

4

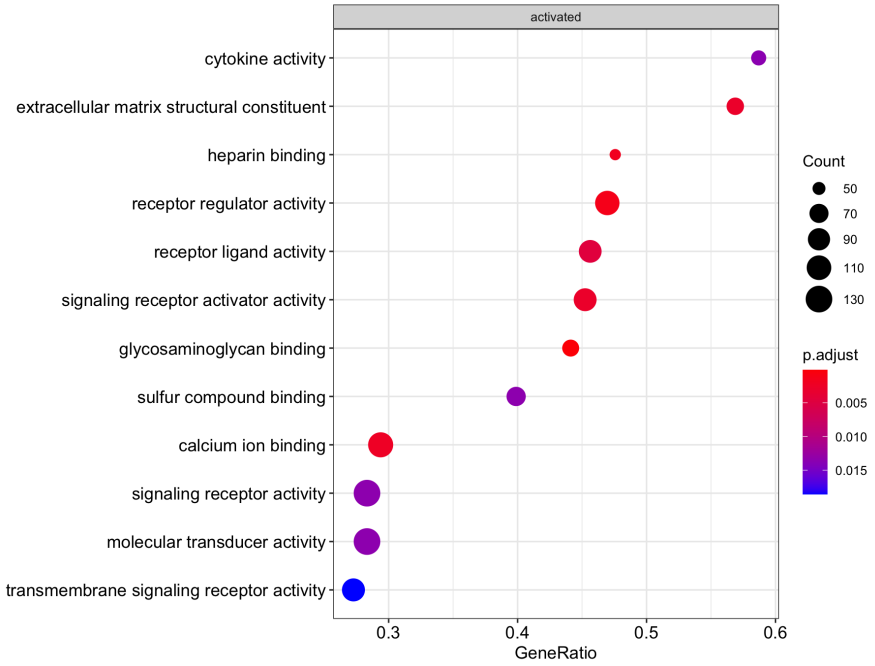

7

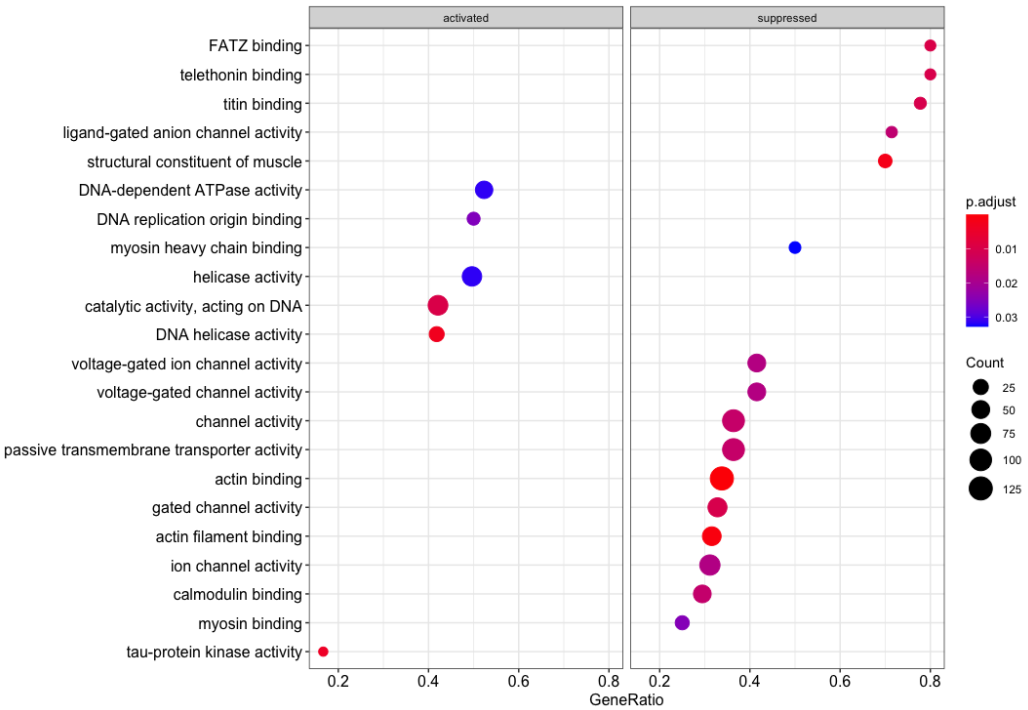

Appendix Figure 4.5 - Molecular Output of Gene Set Enrichment Analysis (GSEA) conducted using Wald test.

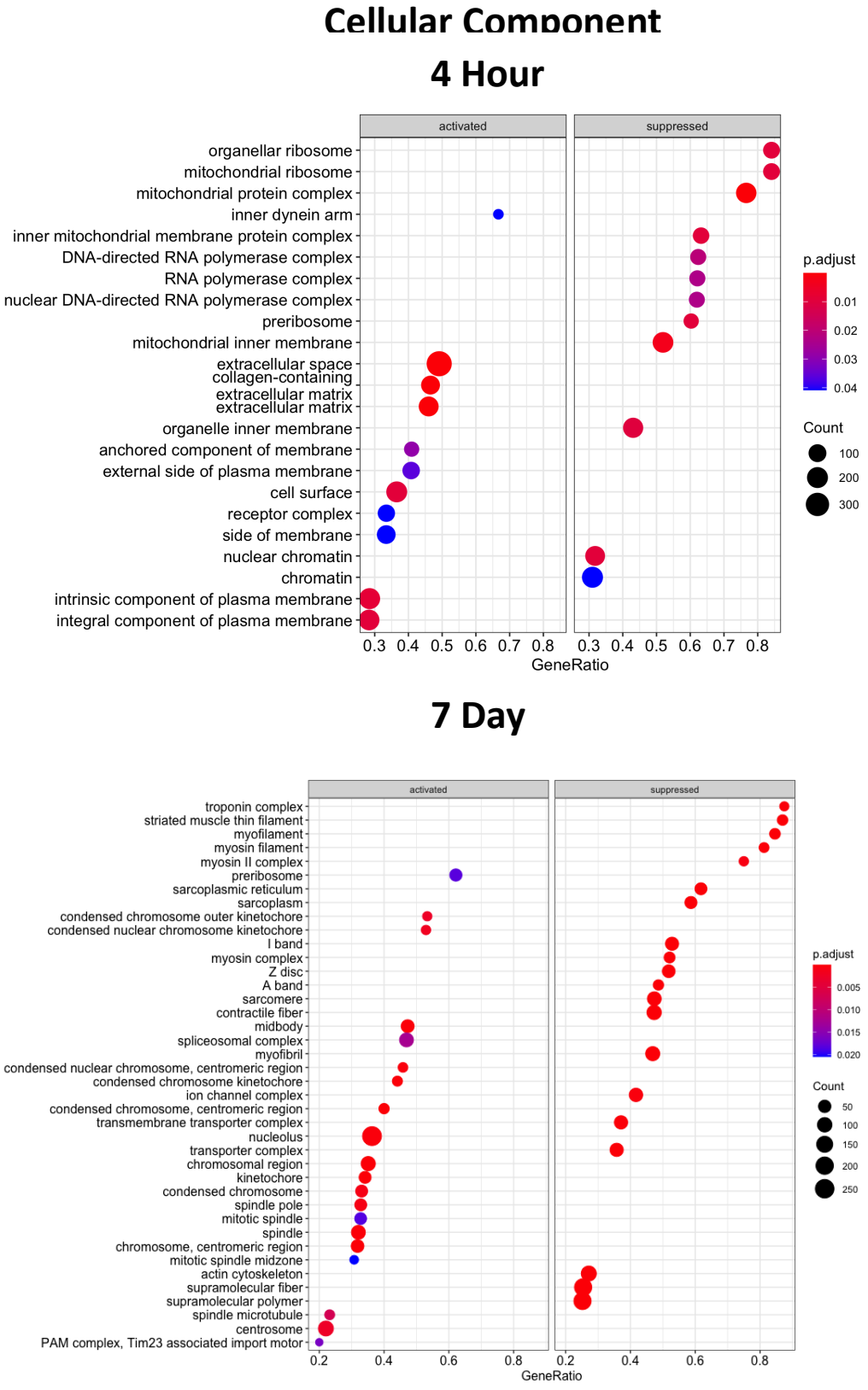

Appendix Figure 4.6 - Cellular Output of Gene Set Enrichment Analysis (GSEA) conducted using Wald test.

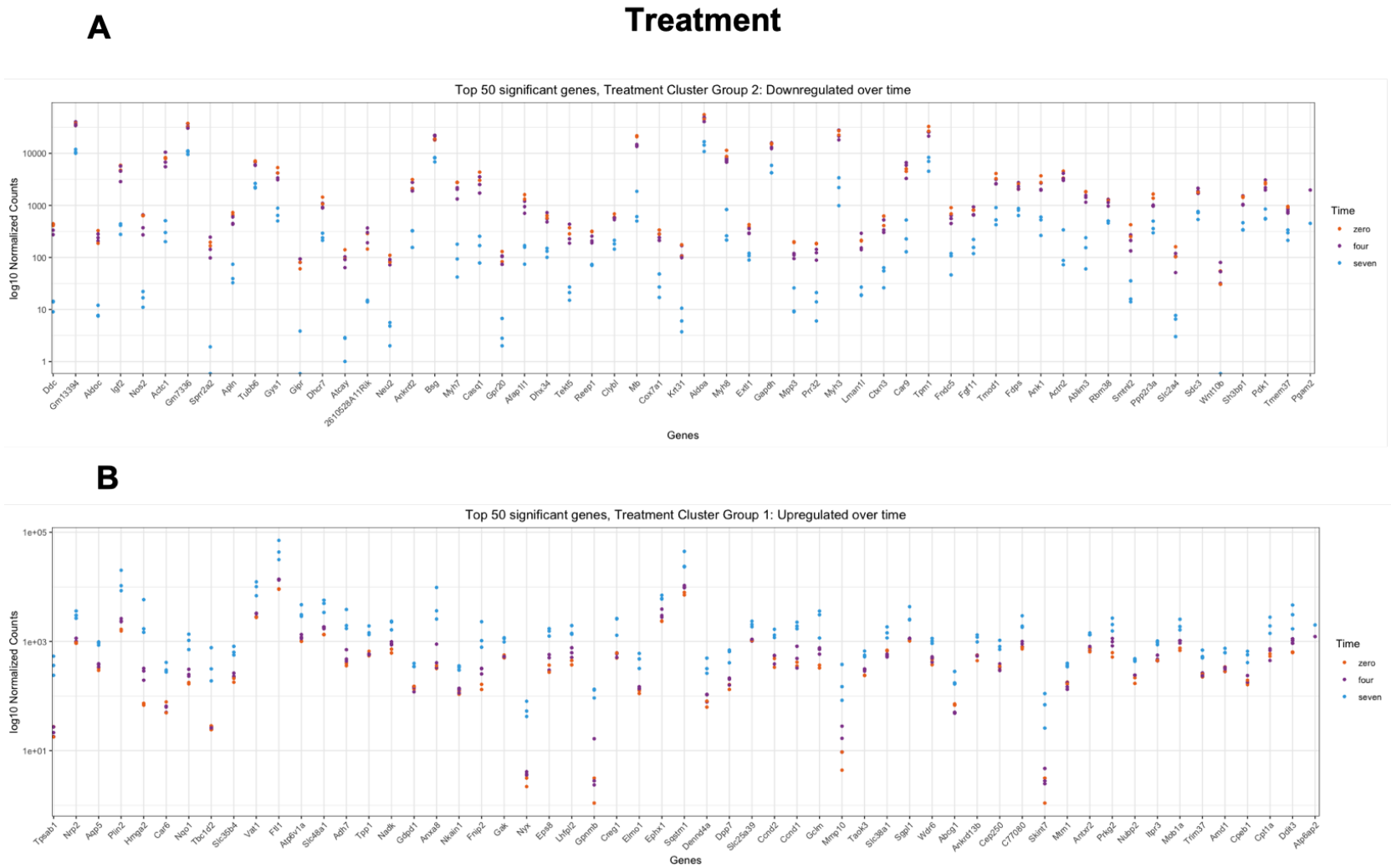

Appendix Figure 4.7 – Top 50 Significant genes in Cluster groups 1 & 2 in the Treatment group.

Control

C

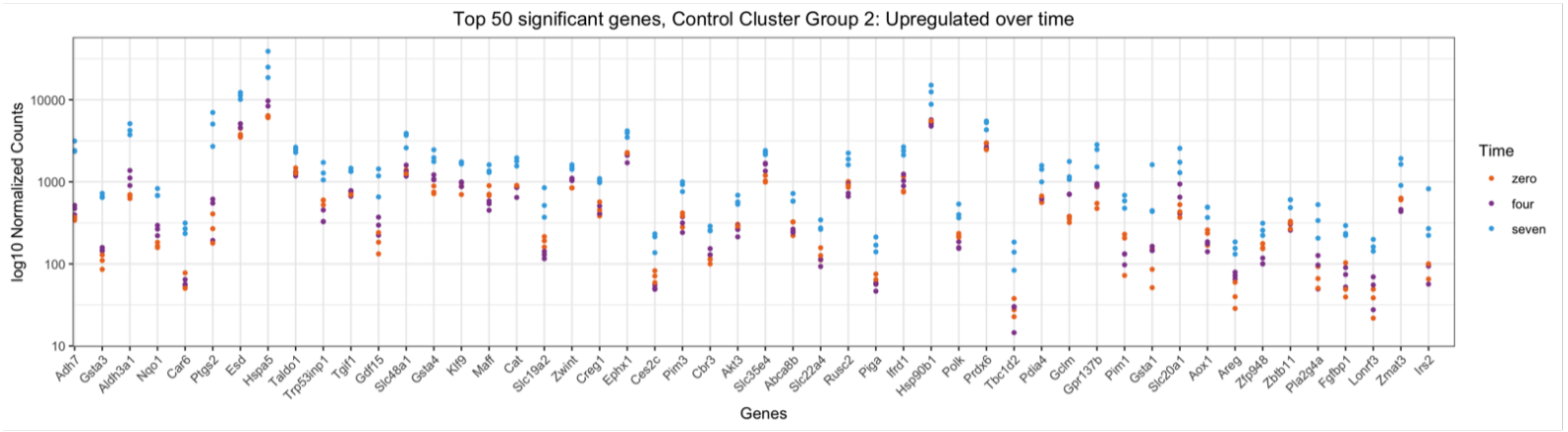

D

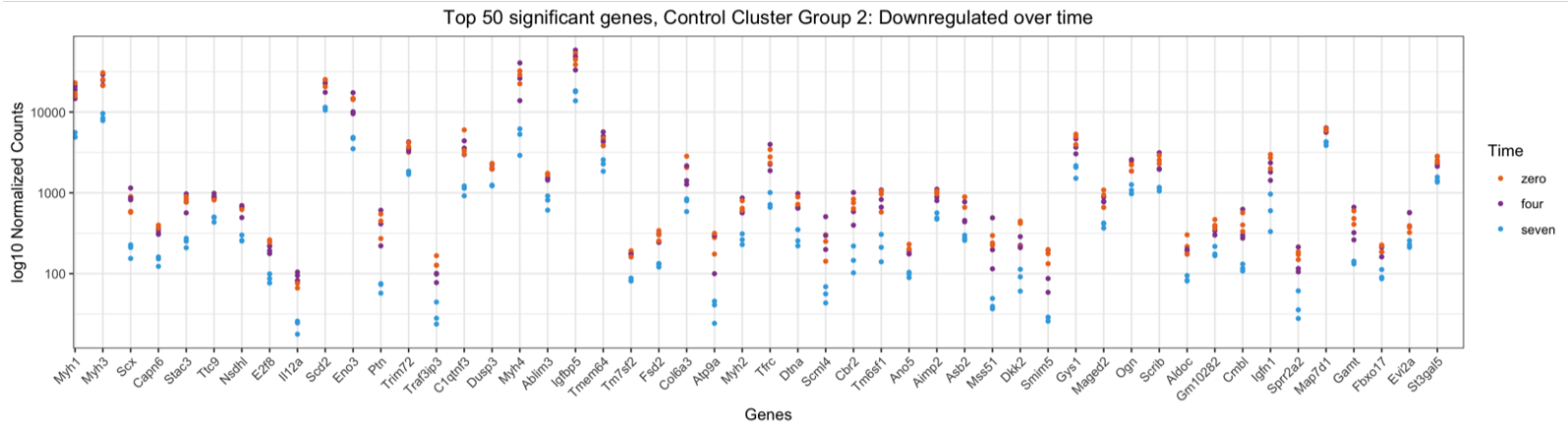

Appendix Figure 4.8 - – Top 50 Significant genes in Cluster groups 1 & 2 in the Control group.

Treatment

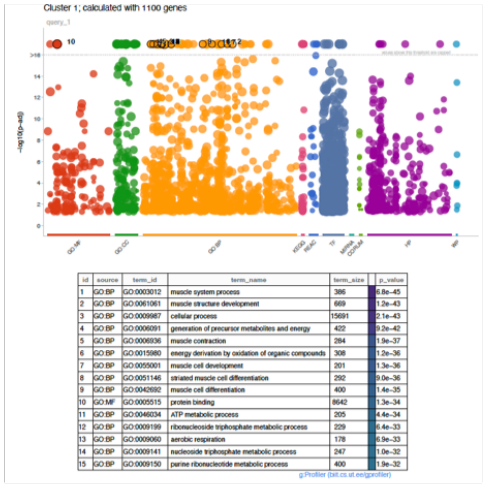

id	source	term_id	term_name	term_size	p_value
1	GO:BP	GO:0003012	muscle system process	386	6.8e-45
2	GO:BP	GO:0061061	muscle structure development	669	1.2e-43
3	GO:BP	GO:0009987	cellular process	15691	2.1e-43
4	GO:BP	GO:0006091	generation of precursor metabolites and energy	422	9.2e-42
5	GO:BP	GO:0006936	muscle contraction	284	1.9e-37
6	GO:BP	GO:0015980	energy derivation by oxidation of organic compounds	308	1.2e-36
7	GO:BP	GO:0055001	muscle cell development	201	1.3e-36
8	GO:BP	GO:0051146	striated muscle cell differentiation	292	9.0e-36
9	GO:BP	GO:0042692	muscle cell differentiation	400	1.4e-35
10	GO:MF	GO:0005515	protein binding	8642	1.3e-34
11	GO:BP	GO:0046034	ATP metabolic process	205	4.4e-34
12	GO:BP	GO:0009199	ribonucleoside triphosphate metabolic process	229	6.4e-33
13	GO:BP	GO:0009060	aerobic respiration	178	6.9e-33
14	GO:BP	GO:0009141	nucleoside triphosphate metabolic process	247	1.0e-32
15	GO:BP	GO:0009150	purine ribonucleotide metabolic process	400	1.9e-32

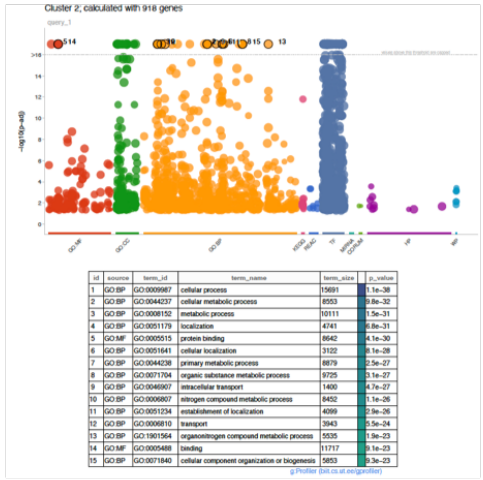

id	source	term_id	term_name	term_size	p_value
1	GO:BP	GO:0009987	cellular process	15691	1.1e-38
2	GO:BP	GO:0044237	cellular metabolic process	8553	9.8e-32
3	GO:BP	GO:0008152	metabolic process	10111	1.5e-31
4	GO:BP	GO:0051179	localization	4741	6.8e-31
5	GO:MF	GO:0005515	protein binding	8642	4.1e-30
6	GO:BP	GO:0051641	cellular localization	3122	8.1e-28
7	GO:BP	GO:0044238	primary metabolic process	8879	2.5e-27
8	GO:BP	GO:0071704	organic substance metabolic process	9725	3.1e-27
9	GO:BP	GO:0046907	intracellular transport	1400	4.7e-27
10	GO:BP	GO:0006807	nitrogen compound metabolic process	8452	1.1e-26
11	GO:BP	GO:0051234	establishment of localization	4099	2.9e-26
12	GO:BP	GO:0006810	transport	3943	5.5e-24
13	GO:BP	GO:1901564	organonitrogen compound metabolic process	5535	1.9e-23
14	GO:MF	GO:0005488	binding	11717	3.1e-23
15	GO:BP	GO:0071840	cellular component organization or biogenesis	5853	3.3e-23

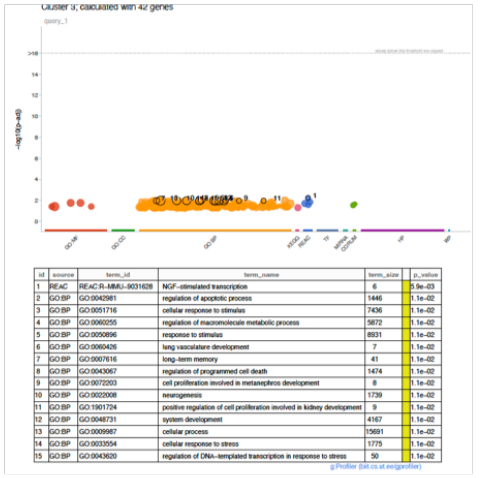

id	source	term_id	term_name	term_size	p_value
1	REAC	REAC:R-MMU-9031628	NGF-stimulated transcription	6	5.9e-03
2	GO:BP	GO:0042981	regulation of apoptotic process	1446	1.1e-02
3	GO:BP	GO:0051716	cellular response to stimulus	7436	1.1e-02
4	GO:BP	GO:0060255	regulation of macromolecule metabolic process	5872	1.1e-02
5	GO:BP	GO:0050896	response to stimulus	8931	1.1e-02
6	GO:BP	GO:0060426	lung vasculature development	7	1.1e-02
7	GO:BP	GO:0007616	long-term memory	41	1.1e-02
8	GO:BP	GO:0043067	regulation of programmed cell death	1474	1.1e-02
9	GO:BP	GO:0072203	cell proliferation involved in metanephros development	8	1.1e-02
10	GO:BP	GO:0022008	neurogenesis	1739	1.1e-02
11	GO:BP	GO:1901724	positive regulation of cell proliferation involved in kidney development	9	1.1e-02
12	GO:BP	GO:0048731	system development	4167	1.1e-02
13	GO:BP	GO:0009987	cellular process	15691	1.1e-02
14	GO:BP	GO:0033554	cellular response to stress	1775	1.1e-02
15	GO:BP	GO:0043620	regulation of DNA-templated transcription in response to stress	50	1.1e-02

Control

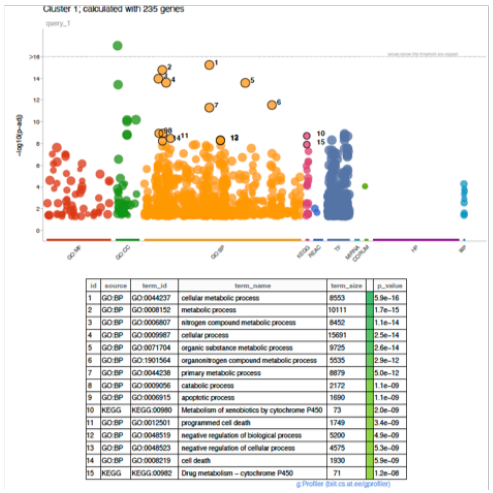

id	source	term_id	term_name	term_size	p_value
1	GO:BP	GO:0044237	cellular metabolic process	8553	5.9e-16
2	GO:BP	GO:0008152	metabolic process	10111	1.7e-15
3	GO:BP	GO:0006807	nitrogen compound metabolic process	8452	1.1e-14
4	GO:BP	GO:0009987	cellular process	15691	2.5e-14
5	GO:BP	GO:0071704	organic substance metabolic process	9725	2.6e-14
6	GO:BP	GO:1901564	organonitrogen compound metabolic process	5535	2.9e-12
7	GO:BP	GO:0044238	primary metabolic process	8879	5.0e-12
8	GO:BP	GO:0009056	catabolic process	2172	1.1e-09
9	GO:BP	GO:0006915	apoptotic process	1690	1.1e-09
10	KEGG	KEGG:00980	Metabolism of xenobiotics by cytochrome P450	73	2.0e-09
11	GO:BP	GO:0012501	programmed cell death	1749	3.4e-09
12	GO:BP	GO:0048519	negative regulation of biological process	5200	4.9e-09
13	GO:BP	GO:0048523	negative regulation of cellular process	4575	5.3e-09
14	GO:BP	GO:0008219	cell death	1930	5.9e-09
15	KEGG	KEGG:00982	Drug metabolism – cytochrome P450	71	1.2e-08

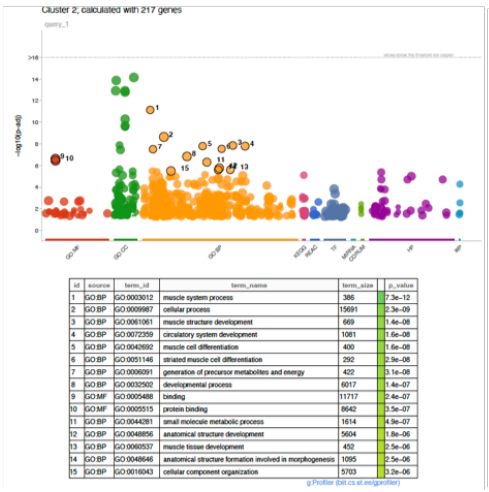

id	source	term_id	term_name	term_size	p_value
1	GO:BP	GO:0003012	muscle system process	386	7.3e-12
2	GO:BP	GO:0009987	cellular process	15691	2.3e-09
3	GO:BP	GO:0061061	muscle structure development	669	1.4e-08
4	GO:BP	GO:0072359	circulatory system development	1081	1.6e-08
5	GO:BP	GO:0042692	muscle cell differentiation	400	1.6e-08
6	GO:BP	GO:0051146	striated muscle cell differentiation	292	2.9e-08
7	GO:BP	GO:0006091	generation of precursor metabolites and energy	422	3.1e-08
8	GO:BP	GO:0032502	developmental process	6017	1.4e-07
9	GO:MF	GO:0005488	binding	11717	2.4e-07
10	GO:MF	GO:0005515	protein binding	8642	3.5e-07
11	GO:BP	GO:0044281	small molecule metabolic process	1614	4.9e-07
12	GO:BP	GO:0048856	anatomical structure development	5604	1.8e-06
13	GO:BP	GO:0060537	muscle tissue development	452	2.5e-06
14	GO:BP	GO:0048646	anatomical structure formation involved in morphogenesis	1095	2.5e-06
15	GO:BP	GO:0016043	cellular component organization	5703	3.2e-06

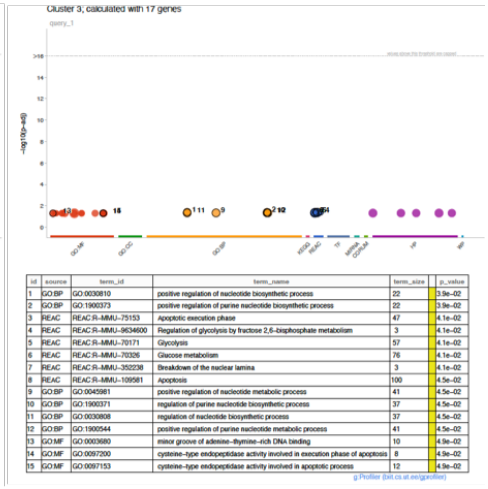

id	source	term_id	term_name	term_size	p_value
1	GO:BP	GO:0030810	positive regulation of nucleotide biosynthetic process	22	3.9e-02
2	GO:BP	GO:1900373	positive regulation of purine nucleotide biosynthetic process	22	3.9e-02
3	REAC	REAC:R-MMU-75153	Apoptotic execution phase	47	4.1e-02
4	REAC	REAC:R-MMU-9634600	Regulation of glycolysis by fructose 2,6-bisphosphate metabolism	3	4.1e-02
5	REAC	REAC:R-MMU-70171	Glycolysis	57	4.1e-02
6	REAC	REAC:R-MMU-70326	Glucose metabolism	76	4.1e-02
7	REAC	REAC:R-MMU-352238	Breakdown of the nuclear lamina	3	4.1e-02
8	REAC	REAC:R-MMU-109581	Apoptosis	100	4.5e-02
9	GO:BP	GO:0045981	positive regulation of nucleotide metabolic process	41	4.5e-02
10	GO:BP	GO:1900371	regulation of purine nucleotide biosynthetic process	37	4.5e-02
11	GO:BP	GO:0030808	regulation of nucleotide biosynthetic process	37	4.5e-02
12	GO:BP	GO:1900544	positive regulation of purine nucleotide metabolic process	41	4.5e-02
13	GO:MF	GO:0003680	minor groove of adenine–thymine–rich DNA binding	10	4.9e-02
14	GO:MF	GO:0097200	cysteine–type endopeptidase activity involved in execution phase of apoptosis	8	4.9e-02
15	GO:MF	GO:0097153	cysteine–type endopeptidase activity involved in apoptotic process	12	4.9e-02

Appendix Figure 4.9 – Gene Set Enrichment analysis data of Control and Treatment LRT gene data.

6

Figure 6.1

Images of shock tube facility

Shock tube and shadowgraph



Shock tube at loading end



Shock tube mouth with target arm



Cell culture mounting apparatus

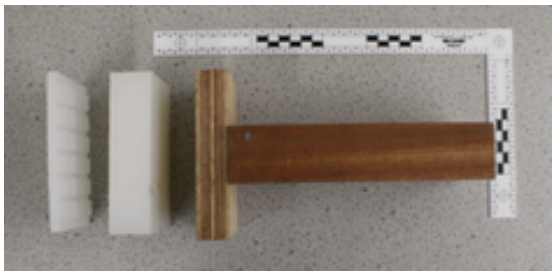

Cell culture mounted on arm in tube



QC Table

Qiacube Protocol for Fibrous Tissue Extraction

1. Add 450 µl ethanol 96-100 % to 900 µl sample lysate supernatant in S-Block
2. Mix 8 x and 1st transfer of 675 µl lysed samples into RNeasy 96 Plate
3. ** Vacuum 25 kPa for 3 min
4. Mix 8 x and 2nd transfer of 675 µl lysed samples into RNeasy 96 Plate
5. ** Vacuum 25 kPa for 3 min
6. *** Add 400 µl RWT into RNeasy 96 Plate
7. *** Vacuum 25 kPa for 1 min
8. ***Add 80 µl DNase-mix into RNeasy 96 Plate
9. *** 15 min incubation
10. *** Add 400 µl RWT into RNeasy 96 Plate
11. *** Vacuum 25 kPa for 1 min
12. Add 600 µl RPE into RNeasy 96 Plate
13. Vacuum 35 kPa for 1 min
14. Add 600 µl RPE into RNeasy 96 Plate
15. Vacuum 35 kPa for 1 min
16. Add 400 µl ethanol 96-100% into RNeasy 96 Plate
17. 2 min incubation
18. Vacuum 35 kPa for 1 min
19. 1 min incubation
20. Drying membrane with vacuum of 50 kPa for 10 min
21. Move transfer carriage to elution position
22 Add 55ul RNase-free Water into RNeasy 96 Plate
23. 5 min incubation
24. Vacuum 35 kPa for 1 min
25. Add 55ul RNase free Water into RNeasy 96
26. Add 30ul TopElute Fluid to into RNeasy 96 Plate
27. 1 min incubation
28. Vacuum 70 kPa for 5 min
29. Move transfer carriage to waste position

----------**

Optional Step: Vacuum performance check after binding step, user confirmation required. Disabled/unchecked by default

*** Optional Step: on-plate DNase digestion. Enabled/checked **** Editable elution parameters

(1) Total Elution Volume: 80–400ul, default = 2x55ul

(2) Elution Steps: 1–2, default = 2

(3) TopElute-Overlay Step: selectable, default = enabled/checked (

3) TopElute-Overlay Step TopElute Fluid can be used during elution of nucleic acids from the RNeasy membrane. It enables application of a stable and high vacuum and results in equal eluate volumes. In addition, TopElute Fluid eliminates the formation of drops of elution buffer at the outlet nozzles of the RNeasy 96 plate. By default, the Top Elute Overlay - option is checked. In case TopElute Fluid should not be used during the run, check the TopElute option under Advanced options. Important: Please ensure that you only take the eluate from below the top layer. Note: TopElute Fluid might be found as a top layer over the elution buffer. It is inert and has no effects on downstream applications